JOURNAL OF AIRCRAFT
Vol. 45, No. 5, September–October 2008

Long-Range Propagation of Sonic Boom from the Concorde Airliner: Analyses and Simulations

Géraldine Ménéxiadis* and Jean Varnier†
ONERA, 92320 Châtillon, France

DOI: 10.2514/1.33899

The reverse problem of finding the position of a supersonic aircraft from infrasound signals recorded at a long distance is dealt with in this paper through analyses of signals generated by the sonic boom of a Concorde aircraft as it was getting close to the French coasts. The signals generated by New York–Paris flights were recorded at very different distances (southwestern France and Normandy). Signals from the southwest were used to define and to test several models (meteorology, propagation, and atmospheric absorption). Signals from Normandy enabled us to apply these models to the reverse problem. Goniometric and spectral analyses associated with these models provide an estimation of the wave train direction and the distance to the sound source, which gives a bearing-and-distance localization of the aircraft. The validation consists of verifying that a reverse ray tracing from the measurement site reaches the aircraft trajectory and that a direct ray tracing launched from this point perpendicularly to the Mach cone can reach the measurement site despite these restricting conditions. In the present study, the calculation of ray paths and Concorde flight data takes account of the Earth's curvature and the weather surveys of the day.

I. Introduction

FOR a long time, the long-range propagation of the sonic boom generated by a supersonic mobile has aroused much interest and research.

Over long distances, a sonic boom degenerates into an infrasonic signal. Man-made infrasound can also be generated by explosions or jet noise. The literature contains numerous examples of infrasound from rocket launches or suborbital vehicle reentries [1,2]. In the case of supersonic aircraft, the N-wave associated with the sonic boom is usually studied at medium distances [3–6]. Long-range infrasonic signals generated by Concorde supersonic airliners flying over the Atlantic have been recorded, for instance, in Sweden [7] and in France [8]. These records and others allow the study of long-range propagation of infrasonic waves through the atmosphere. The infrasounds detected have a continuous background noise coming from natural sources such as wind, ocean waves, volcanoes, etc. [9,10]. Of course, the infrasonic wave propagation depends on meteorological conditions and, more specifically, on the stratospheric wind profiles. For instance, acoustic signals received in the northeastern coastal regions of the United States from rockets launched at Cape Canaveral show strong seasonal effects [11]. Several models concerning the atmospheric absorption can be found in the literature [12]. The atmospheric effects on the shape and the propagation of sonic boom are more particularly studied in [13,14]. Absorption increases with frequency and becomes really important at an altitude higher than 100 km. Therefore, infrasound can be propagated at a long distance, whereas trajectories at very high altitudes keep only very low frequencies that may vanish in the natural background noise.

At ONERA, we have a set of infrasound signals recorded on the southwestern coast of France and in Normandy. These signals are those of New York–Paris Concorde flights over the North Atlantic. Our 3-D ray simulations taking into account weather conditions and the Earth's curvature (see also [15,16]) allowed us to link the source model and the final direction of the sound waves. To compare its final shape with the recorded signal spectrum, we also simulated the distortion of the N-wave spectrum envelope due to the atmospheric attenuation according to the distance. Finally, long-range 3-D-ray reverse simulation and associated N-wave spectrum distortion allowed us to give a rough estimation of the position at which the sonic boom was emitted.

II. Flight Data

The signal analyzed in this paper concerns the Concorde Air France flight AF001 from New York (JFK airport) to Paris (CDG airport). Trajectory, schedule, and other flight data were provided by former pilots of Concorde. The AF001 flight used to leave New York in the morning and land in Paris at 1645 hrs Greenwich Mean Time (GMT), plus or minus 15 min. In Fig. 1, we can see that the air corridor in approach of Brittany (westernmost coast of France) included two turning points (called BISKI and GUR) about 216 n mile apart. According to the AF001 flight plan, the air-corridor azimuth was 100 deg on arriving at BISKI and 83 deg on leaving. Concorde was flying at around 57,000 ft with a cruise speed of Mach number $M = 2$. Of course, its turn trajectory differed from the theoretical route (Fig. 2). At about 50 n mile after BISKI, the aircraft started to decelerate and descend. Its speed became subsonic at 40 n mile before GUR (Guernsey Island). Let us note that the approach azimuth toward GUR is 86.5 deg and not 83 deg due to the Earth's curvature, because the air corridor follows an orthodromy (i.e., the path along a great circle centered at the Earth's center). It should be noted that the projection on the Earth's surface of a ray trajectory through a standard layered atmosphere also follows an orthodromy.

III. Signals Recorded on the Southwestern Coast of France

A. Signal Analysis

Here, we considered the signals recorded on 17 March 2003, between 1600 and 1630 hrs GMT with an array of 6 sensors. The infrasound measurement site was located on the Atlantic coast in southwestern France, about 600 km south of Guernsey (Fig. 1). The acquisition frequency was 100 Hz. The unfiltered signal including the natural background noise is shown in Fig. 3a.

To determine the inbound direction (azimuth θ and elevation φ) of sound waves received, we correlated the sonic boom signal (useful signal). To this end, knowing that the background noise predominates at very low frequencies (Fig. 4), we decided to filter

Received 6 August 2007; accepted for publication 6 May 2008.

*Ph.D. Student, Department of Numerical Simulation and Aeroacoustics.
†Research Engineer, Department of Numerical Simulation and Aeroacoustics.

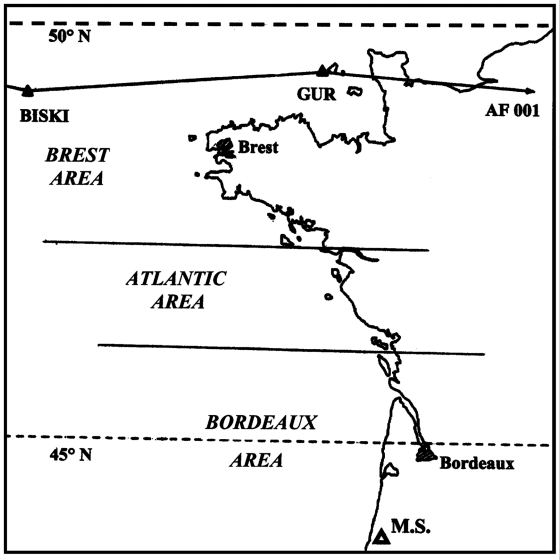

Fig. 1 Concorde AF-001 air corridor with meteorological areas selected.

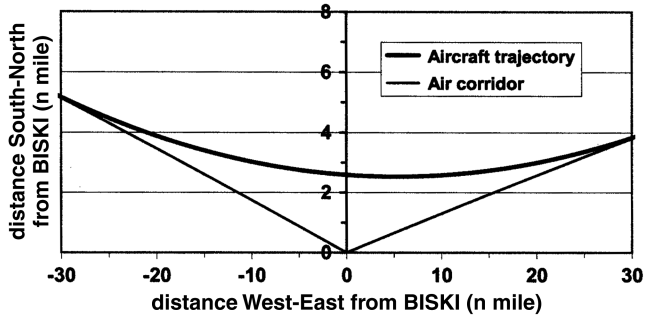

Fig. 2 Air corridor and aircraft trajectory at BISKI turning point.

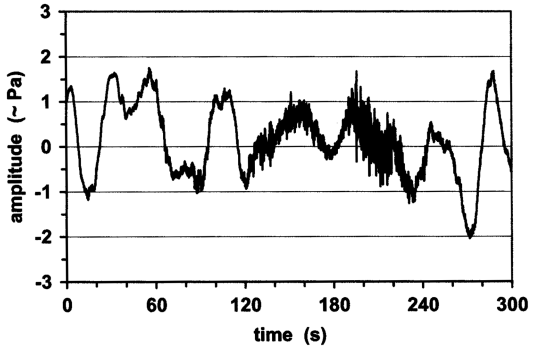

a)

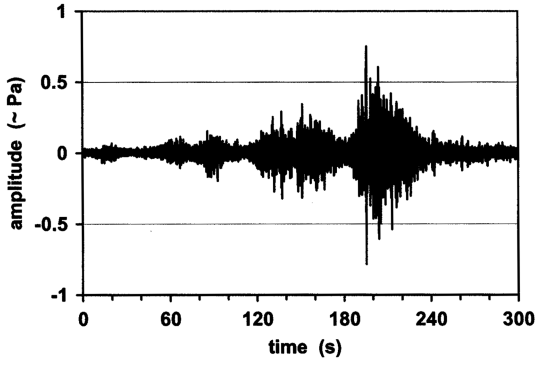

b)

Fig. 3 Sound pressure signal from the Concorde: a) unfiltered and b) 1.5 Hz high-pass-filtered.

out the signal below 1.5 Hz (however, we could have selected another frequency close to 1 Hz) (Fig. 3b). Using several time windows, we found an azimuth angle θ such as $320\,\text{deg} < \theta < 324\,\text{deg}$. Unfortunately, the acquisition frequency was too low or the sensors were too close to each other for an accurate calculation of the apparent sound speed giving the wave incidence. For instance, for two sensors roughly aligned in the signal azimuth, we obtained a maximum correlation at two successive sampling steps (0.01 s). Thus, the apparent propagation speed appears to be close to either the ambient sound speed (343 m/s) or the slightly supersonic speed (365 m/s), which gives elevation angles $\varphi \approx 0\,\text{deg}$ (grazing incidence) and $\varphi \approx 20\,\text{deg}$, respectively. It is interesting to note that the inbound direction of sound wave trains does not vary significantly but oscillates around an average value during the three useful minutes of the signal. Therefore, we can suppose that these wave trains are only duplications or echoes of a unique initial pulse (near Concorde flying at Mach 2, the N-wave does not last over 0.1 s), which may be explained by the very directional character of the Mach cone. About the signal duplication, we know that thunderbolts and detonations also give rise to a rumble, the duration of which increases with the distance from the source. This phenomenon is partly related to acoustic diffraction in the ground vicinity [17].

Spectral analyses of the signal in successive time windows seem to confirm this redundancy, with differences between the spectra having an apparently random character. For this reason, it was necessary to smooth the signal by calculating an averaged spectrum. The same method was applied to the background noise. To avoid a loss of information below 1.5 Hz, our preference went to analyzing the unfiltered signal rather than the filtered one. The background-noise spectrum (see Fig. 4) results from spectral analyses of five successive time windows with no useful signal (60 s each). The unfiltered-signal spectrum results from spectral analyses of five successive time windows with a useful signal (12 s each). Figure 4 shows that the useful signal emerges from the background noise in the frequency range of 1–10 Hz. We know that only frequencies less than 1 Hz can spread over the thermosphere. Thereby, this spectrum shape clearly indicates a stratospheric propagation (altitude $z < 60$ km).

B. Three-Dimensional Ray Simulations

We used a classical 3-D ray propagation model based on the principles of geometrical acoustics. We knew that this tool allows a fast calculation of long-range trajectories, but it is quite imperfect, because wave frequency and atmospheric diffraction effects are not taken into account. The numerical computation is based on a finite difference method, the stability of which was checked at various computation Δt steps for distances of several hundred kilometers. The value $\Delta t = 0.02$ s allows a quick and precise calculation of propagation time and trajectory length. The meteorological conditions of the day are given 1) up to the altitude $z = 28,000$ m by time-interpolated weather surveys at 1200 and 2400 hrs GMT from radiosonde stations at Bordeaux and Brest (see Fig. 1) and 2) over 35,700 m by the Committee on Space Research (COSPAR)

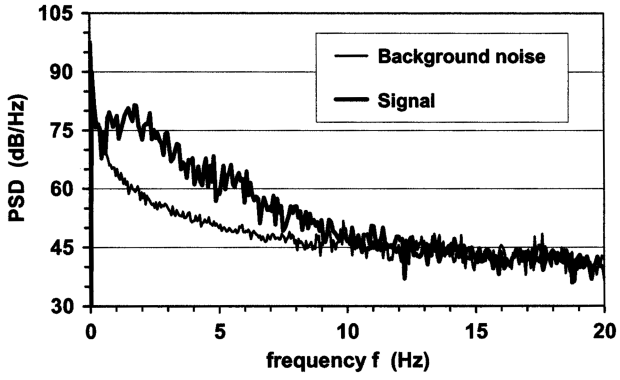

Fig. 4 Background noise and unfiltered-signal spectra.

International Reference Atmosphere, providing seasonal averaged data for the 45th and 50th north parallels.

In the Brest area, we used the weather data from Brest and the COSPAR data of the 50th north parallel. In the Bordeaux area, we used the weather data from Bordeaux and the COSPAR data of the 45th north parallel. Moreover, around the measurement site, we adopted the local weather survey given from ground level up to 1500 m in height. We added an intermediate Atlantic area, averaging the weather data of the Brest and Bordeaux areas.

To be more realistic, a degree of freedom called the wind factor allowed us to modify the COSPAR wind data in proportion. In the linking zone between 28,000 and 35,700 m, the wind and temperature data are linearly interpolated. To reduce the gap in the linking zone between the recorded and the statistical wind data, we used average winter COSPAR data between January and March. However, the resulting wind profile shown in Fig. 5 also suggested introducing a wind factor greater than 1. Please note that there is no gap for temperature in the linking zone.

The algebraic model was in Cartesian coordinates, but it was necessary to take into account the Earth's curvature for the sound ray computation. The Mercator projection keeps the true value of the angle between wind direction and meridians, but in such a projection, an orthodromy becomes a curved line. Analytical calculation shows that at the latitudes we considered, the orthodromy azimuth increases of about 1 deg for 100 km in the west–east direction (see, for instance, the initial and final azimuths of the BISKI–GUR air corridor). Moreover, the Earth's great circle curvature is 360 deg for 40,000 km in circumference (i.e., 0.9 deg for 100 km). Therefore, a straight trajectory in real space becomes a curve in the third dimension of Mercator space. Finally, to calculate a ray trajectory more or less accurately, we must modify the direction of the wave vector step by step with the following ratios: $+1$ deg for azimuth θ for 100 km eastward and $+0.9$ deg for elevation φ for 100 km on orthodromy.

The projection of the ray trajectory on the Mercator plane is slightly greater than the orthodromy, because the wind is not constant according to the altitude. In this plane, it is necessary to consider an average distance between the meridians, including the trajectory. The result is validated by comparing the orthodromic length calculated directly in spherical coordinates with the projection length calculated step by step in the Mercator plane.

The direct 3-D ray simulations are made from arbitrary points of the aircraft trajectory to estimate the value of the unknown wind factor in the upper atmosphere, knowing that this value is probably greater than 1. The rays are emitted perpendicularly to the Mach cone, the spread angle α of which is 30 deg at Mach 2. This source model is very restricting, because azimuth θ and elevation φ of a ray are correlated via α. To reach the measurement site (MS), a ray must be emitted toward the stratosphere with a wind factor empirically set at 1.05. The emission point must be located at a short distance after BISKI. The MS is reached at the third reflection on the sea surface (Fig. 6), knowing that incidence and reflection angles are set by the wave-vector direction. Here, the trajectory height is 45 km, its duration is 40–30 min, and its length is close to 800 km for a

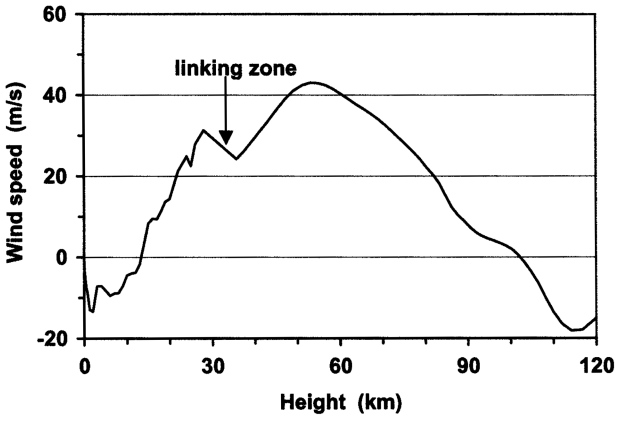

Fig. 5 West–east component of the wind speed in the Brest area.

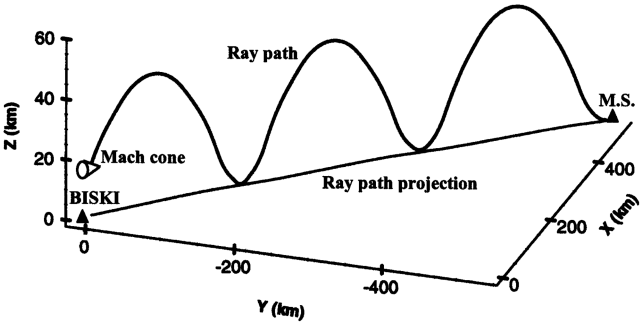

Fig. 6 Three-dimensional ray tracing from the aircraft to the measurement site.

projection length of 740 km (the orthodromic length between BISKI and the MS is 737 km). The wave-vector azimuth increases along the trajectory from 316 to 321 deg, in accordance with the experiment, as well as the flying time calculated at BISKI. The incidence angle at the MS is, in fact, close to 0 deg.

Let us note that we can also reach the MS after four reflections with rays directly emitted toward sea level (sonic boom primary carpet). The trajectory height is 44 km, its duration is 42 min, and its length is 812 km for a projection length of 748 km. For that, the wind factor must be set at around 1.3, which is a strong but possible value. Indeed, British weather surveys recorded in February up to 60,000 m in altitude show that the average values of the wind factor for altitudes over 30,000 m generally remain between 0.5 and 1.5.

It is well known that the ray trajectories are not reversible in the presence of wind gradients [18]. Nevertheless, it is possible to obtain retrograde trajectories by reversing the wind direction at all altitudes. Computations made from the MS with a set of initial directions (θ, φ) show that the trajectories remain stratospheric if $\varphi < 15$ deg, but that the aircraft trajectory can be reached at the flight altitude only for $\varphi < 5$ deg. For some values of θ, the third reflection occurs west of BISKI, but these trajectories are not compatible with the Mach-cone direction. Finally, the reverse ray simulation indicates that only the small part of aircraft trajectory found by direct simulation can be taken as a sound source.

C. N-Wave Spectrum Distortion

We know that the forward and rear shock fronts of a theoretical N-wave of width T are responsible for the well-known arched shape of its sound power spectral density (PSD). Let us note that the slope of its envelope (≈ -6 dB per octave above the frequency $f = \sqrt{3}/\pi T$), linked up to an equation in $1/f^2$, does not depend on length or width of the N-wave (see Fig. 7). As indicated in [19], the slope of a real N-wave spectrum envelope is -12 dB per octave above the break point at $f = 1/\pi\tau$, where τ is the rise time (see

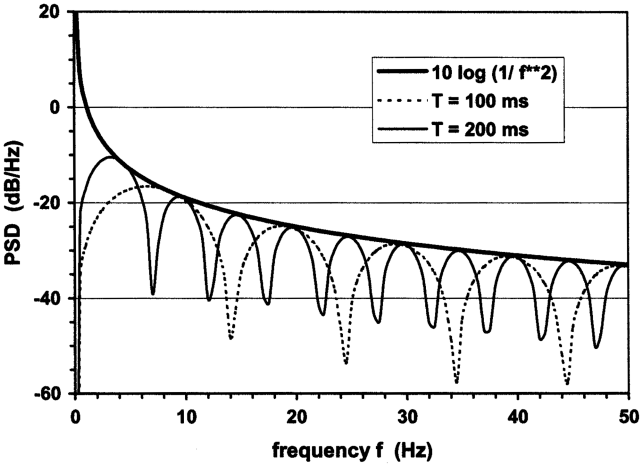

Fig. 7 Spectra of 2 N-waves of different widths and their common envelope.

Fig. 8). In fact, the rise time of a shaped sonic boom is very short, which gives a break point in the sonic range, widely outside the infrasound range. See, for instance, [20], in which the slope of the spectrum of the sonic boom recorded at some ten kilometers from Space Shuttle *Columbia* in approach flight ($M < 1.5$) remains equal to −6 dB per octave (−20 dB per decade) from 2 to 50 Hz at least. Mainly due to atmospheric absorption effects, the N-wave shape degenerates with the propagation distance and becomes smoother. As a result, the spectral minimums are attenuated and become indiscernible at a great distance. Yet our hypothesis is that the spectrum is degraded less than the time signal. More precisely, we assume that the signal spectrum shape follows the slope of the N-wave spectrum envelope. This envelope is deduced from the initial envelope of Fig. 7 by subtracting the atmospheric absorption that increases according to the frequency and the propagation distance. The curve of atmospheric absorption of Fig. 9 is obtained by averaging Sutherland's coefficients [12] between $z = 0$ and 60 km (note that the air may be considered as dry above 12,000 m). Then the 3-D ray code calculates the attenuation step by step along the ray path at every frequency and cumulates it at every reflection. The N-wave spectrum envelope resulting from this attenuation is shown here at the third reflection after 800 km of trajectory (Fig. 10). The envelope follows the signal spectrum shape in a satisfactory manner, except for the lowest frequencies, as suggested by Fig. 7. Of course, this is not true above 10 Hz, where the background noise predominates (see Fig. 4). Let us note that the background-noise spectrum follows a natural slope in $1/f^2$ (−6 dB per octave), as does the initial envelope of the theoretical N-wave spectrum (0-km curve in Fig. 10).

IV. Signals Recorded in Normandy

A. Spectral Analysis and Direction-Finding

We proceeded in the same way for other signals recorded on 15 November 1999, from 1620 hrs GMT. The MS is located in Normandy at around 200 km east from Guernsey, at an altitude of 200 m above sea level.

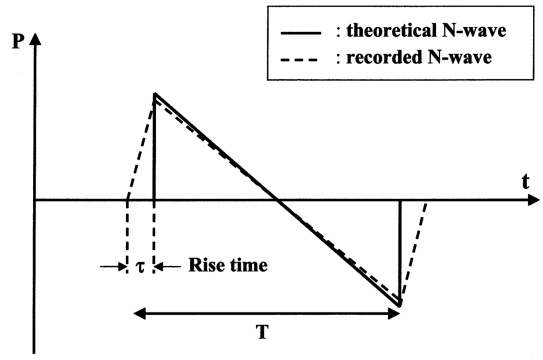

Fig. 8 Idealized N-wave and realistic shape of a sonic boom.

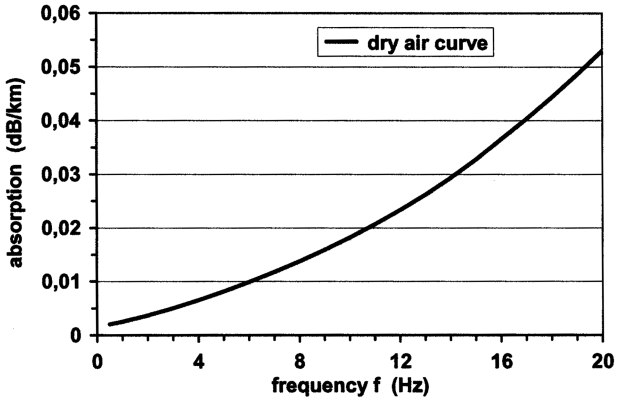

Fig. 9 Averaged atmospheric absorption deduced from [12].

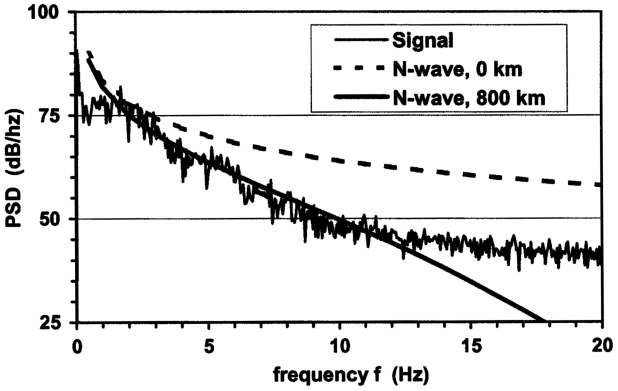

Fig. 10 Signal spectrum recorded in southwestern France; N-wave spectrum envelopes.

We used signals recorded by four sensors at a sampling frequency of 20 Hz. The distance between two sensors was 1 km or more. To suppress the main component of background noise, the signal was filtered at 0.5 Hz. In this paper, we only examine the main signal series that lasts 36 s, divided for our analyses in three periods of 12 s. The spectral analyses are made in the frequency range of 0.5 to 8 Hz, with a signal-to-noise ratio of 10 dB or more. In each window, the smoothing process was as follows: 1) time average of the spectra of four windows of 3 s for each sensor and 2) spatial average of the resulting spectra of the four sensors.

The first process is a quadratic average made in Pa^2/Hz to detect the possible valley points of an N-wave spectrum. The second is an artificial smoothing made in decibels/hertz, to suppress the small random peaks and to reduce the influence of local level differences between sensors. For each period, the arches of the resulting spectrum are not discernible, but this spectrum oscillates around the theoretical N-wave spectrum envelope after 300 km of atmospheric propagation (Fig. 11). This envelope and the others were directly deduced from the initial envelope of the N-wave using the averaged absorption coefficients shown in Fig. 9, without resorting to weather conditions and ray tracing. It should be noted that the significant datum taken into account for this comparison is the spectrum slope and not the spectrum level. Thus, the result does not really depend on the signal-to-background-noise ratio.

Next, for the same periods of 12 s, we made analyses to determine the reception angles (θ, φ) of the wave trains. The correlation functions were calculated between the six pairs formed by the four sensors S1 to S4. With the unfiltered signals, this operative mode allowed us to observe inconsistencies between the computed propagation times for every sensor pair, probably due to the local wind influence. In contrast, the propagation times were very coherent by using the filtered signals (Fig. 12), which allowed a precise calculation of the inbound direction of the wave vector. Thus, we notice that azimuths θ are similar (285.5 deg $\pm$ 0.5 deg) and that elevations φ are close to zero (less than 2 deg), the apparent wave

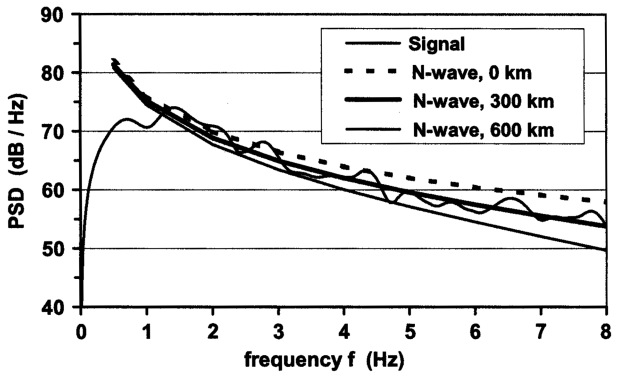

Fig. 11 Signal spectrum recorded in Normandy; N-wave spectrum envelopes.

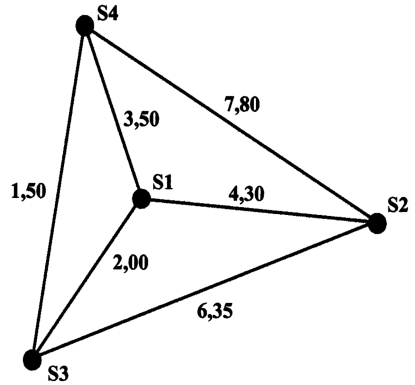

Fig. 12 Propagation times (in seconds) deduced from the maximum values of the correlation functions.

velocity between the sensors being close to the ambient sound velocity.

Let us note that the preceding is a rough estimation of the sound-source position from azimuth and distance calculation.

The use of the averaged absorption coefficients to estimate the horizontal distance to the sound source implies several approximations. In particular, we neglected the real shape and height of the ray paths, because this model actually amounts to considering a propagation in the broken line between 0 and 60 km in altitude. Note that the strong absorption at high altitude is compensated here by a short travel time, which is not the case for real sound wave trajectories. However, the use of the nominal coefficients along a ray path underestimates the atmospheric absorption for low-altitude trajectories, such as those of Sec. III. Therefore, we can suppose that other phenomena, such as the damping of the nonlinear effects, intervene to increase the spectrum distortion at a long distance.

B. Flight Data and Mach Cone

The time schedule of the signals recorded on 15 November corresponds to the fly pass over the English Channel by the Concorde aircraft (Flight Air France 001). The approach trajectory toward Guernsey was reconstructed by a former pilot of Concorde according to the flight tables and to the weather surveys of that day (meteorological station of Brest, Brittany). The aircraft decelerates from Mach 2 to 0.95, following a shallow descent of about 200 km up to the flight level 32,000 ft. The deceleration is more or less constant, and the trajectory slope varies between 0 and −5 deg. Concerning the latter data, we note that the axis of the Mach cone is determined by the aircraft trajectory and not by the aircraft attitude.

We have simulated the distortion of the Mach cone due to the deceleration by assuming a constant deceleration and a constant sound speed, which is almost true in the altitude range considered. By neglecting the nonlinear effects (cone spread given by $\sin\alpha = 1/M$, where M is the local Mach number), we made an analytical calculation from kinematic data. We calculate the shock-front development in a horizontal plane with a step of 100 s, between Mach 2 and Mach 1. Results are shown in Fig. 13. The aircraft speed becomes sonic at coordinates (0,0). From this moment, the sound propagation becomes quasi-spherical, and the aircraft flying at a subsonic speed comes off the wave front (triangle in Fig. 13). Let us note that a given wave vector remains normal to this front. Thus, the inbound direction of the wave vector indicates the sound-source position on the aircraft trajectory, as in the case of constant Mach number.

C. Reverse and Direct Ray Calculations

The retrograde rays are launched from the MS at 200 m above sea level, following angles θ and φ determined for the three time periods of 12 s, and are stopped in the vertical plane containing the aircraft trajectory. Remember that this reverse calculation requires the wind inversion at all altitudes. For high altitudes, the COSPAR data used

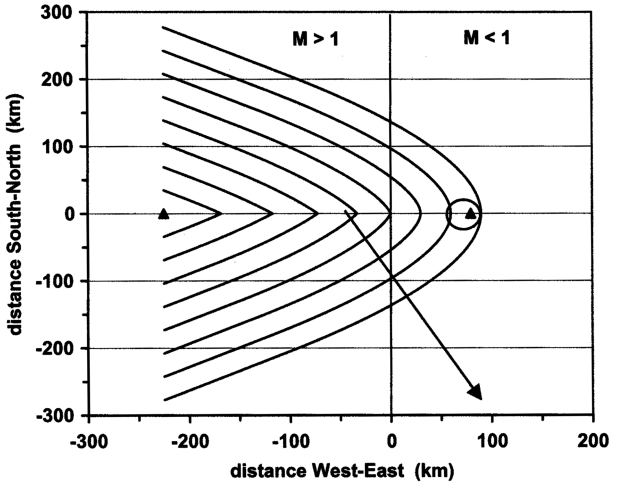

Fig. 13 Wave-front development in deceleration, with a time step of 100 s.

are those of the 50th north parallel in November. For medium and low altitudes, we use weather data from meteorological stations of Brest and Trappes (near Paris), with an interpolation according to the longitude of every point we consider. Around the MS, we use the local weather survey given from ground level to 1500 m in height. The wind profile shown in Fig. 14 suggests us that the wind factor of COSPAR data may be close to 1.

As we can see in Fig. 15, the retrograde rays corresponding to the three time periods cross the aircraft trajectory at more or less suitable altitudes after reflections at around 40 and 0.9 km above sea level. The wind factor was set to 1 by default, which seems to be a convenient value for this simulation. The travel times oscillate around 15–20 min, and the three points of arrival are within 10 km along the aircraft trajectory and within 6 km in height. The curvilinear distance of propagation is very close to 300 km, in accordance with the rough estimation stemming from the spectral

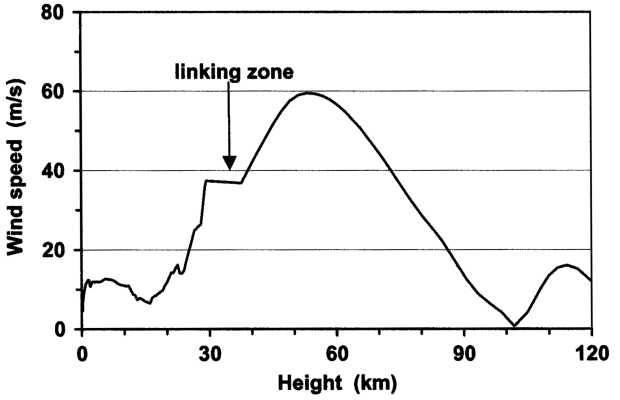

Fig. 14 West–east component of the wind speed over Normandy's measurement site.

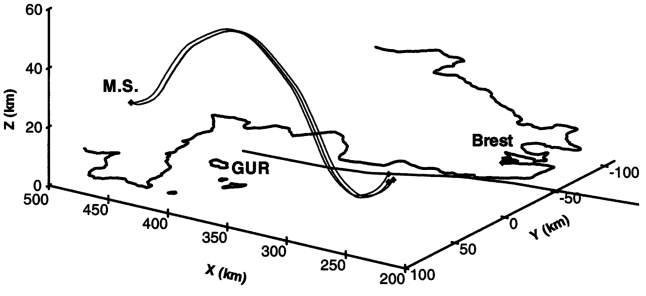

Fig. 15 Reverse ray tracing from the measurement site; aircraft trajectory.

analysis. The horizontal projection of the ray path gives an emission point of the sonic boom at around 280 km from the reception point. Thus, there is a difference of less than 10% between the curvilinear length of ray path and the orthodromic distance between the sound source and the hearing point. This is true, in general, in the case of a stratospheric propagation, which allows us to assimilate curvilinear and horizontal distances.

At the interception points by the retrograde rays, the Concorde aircraft is in descent flight with a slope of −3.7 deg and its speed is close to Mach 1.20. We know that these data do not intervene in our reverse method, but allow us to define the local Mach cone used to start the direct ray calculation. We find a suitable direct ray tracing (that well reaches the measurement site with a grazing incidence) in the part of the preceding determined aircraft trajectory, which confirms the accuracy of the reverse calculation, including the direction-finding. The direct ray path is very close to the paths of the retrograde rays. However, it is important to notice that a single ray of this kind can be found. This fact seems to confirm that the useful signal analyzed was caused by a single pulse. Actually, we know that all physical phenomena are not taken into account by our propagation model, particularly in the infrasound field.

V. Conclusions

In the two cases that we studied, we developed two methods to analyze long-range signals generated by aircraft sonic booms.

Reverse ray simulations, linked up with goniometric analyses of the recorded signals to determine the wave train directions, allowed us to find the part of the Concorde aircraft trajectory from which the sonic boom was emitted. From this trajectory part, knowing the local flight data accurately, it was possible to reach the measurement site with a direct ray emitted perpendicularly to the Mach cone, which constitutes a very restricting condition, because a single emission point may be found. In relation to the maximum height of the meteorological surveys of the day, the COSPAR seasonal weather data were used above 30 km in altitude, with minor changes of the wind speed.

The other method that may be associated with the goniometric analysis consists of calculating the distortion of the envelope of a theoretical N-wave spectrum by the atmospheric absorption, to compare this envelope with the signal spectrum and to estimate the propagation distance. For that, we assume that this spectrum is degraded less than the time signal. We find a satisfactory agreement between the resulting envelope and signal spectrum shape at distances of around 300 and 900 km from the measurement sites.

The latter method may be used without knowing aircraft trajectory, flight data, and (in a first approach) weather conditions. However, the use of absorption coefficients averaged between 0 and 60 km in altitude implies a stratospheric propagation of sound, generally revealed by a frequency range spreading over 1 Hz. It seems that this process may overestimate the atmospheric absorption in some cases, yet the results are satisfactory in the two cases examined. Thus, we are able to roughly estimate the emission point of an aircraft sonic boom from bearing-and-distance data and to specify it by making a reverse ray calculation if the weather conditions and the flight data are known.

It is interesting to notice that these calculations do not depend on the measured sound levels and, in some limits, on the signal-to-background-noise ratio. To our knowledge, both methods of spectrum-shape analysis at long distances and of reverse ray calculation with wind inversion are not quoted in the related literature. Recent research [21,22] is mainly focused on other types of infrasound sources such as explosions, the localization of which is mainly based on azimuth crossing, sound-level calculation, and time–frequency analysis, which often involves several hearing sites or the detection of multiple ray paths.

The difficult points in the classical localization methods used concern the knowledge of weather conditions, the calculation of sound intensity and of atmospheric absorption, and the influence of shadow zones and other acoustic phenomena such as the diffraction. In contrast, subject to an appropriate setting of the absorption curve according to the frequency, a method mainly based on the spectrum-shape distortion avoids most of these difficulties.

We now have to test the limits of this method with infrasound signals from Concorde recorded at 3000 km away or more.

Acknowledgments

This study was supported by Commissariat de l'Energie Atomique (CEA), Bruyères-le-Châtel, France, and ONERA, Châtillon, France, in the frame of a work directed by Jean-Pierre Sessarego, Centre National de la Recherche Scientifique (CNRS), Marseille, France. The authors greatly appreciate Pierre Grange and Gérard Duval, former pilots and instructors of Air France Concorde, as well as Philippe Delorme and Charles-Jean Deléris for their helpful collaboration.

References

[1] Balachandran, N. K., and Donn, W. L., "Characteristics of Infrasonic Signals from Rockets," *Geophysical Journal of the Royal Astronomical Society*, Vol. 26, 1971, pp. 135–148.

[2] Kaschak, G., Donn, W. L., and Fehr, U., "Long-Range Infrasound from Rockets," *Journal of the Acoustical Society of America*, Vol. 48, No. 1, Pt. 1, 1970, pp. 12–20. doi:10.1121/1.1912102

[3] Norris, R. N., Haering, E. A., Jr., and Murray, J. E., "Ground-Based Sensors for the Sr-71 Sonic Boom Propagation Experiment," NASA TM 104310, Sept. 1995.

[4] Ivanteyeva, L. G., Kovalenko, V. V., Pavlyukov, E. V., Teperin, L. L., and Rackl, R. G., "Validation of Sonic Boom Propagation Codes Using Sr-71 Flight Test Data," *Journal of the Acoustical Society of America*, Vol. 111, No. 1, Pt. 2, Jan. 2002, pp. 554–561. doi:10.1121/1.1404377

[5] Plotkin, K. J., "State of the Art of Sonic Boom Modeling," *Journal of the Acoustical Society of America*, Vol. 111, No. 1, Pt. 2, Jan. 2002, pp. 530–536. doi:10.1121/1.1379075

[6] Plotkin, K. J., Page, J. A., Graham, D. H., Coen, P. G., Haering, E. A., Maglieri, D. J., et al., "Ground Measurements of a Shaped Sonic Boom," 10th AIAA/CEAS Conference, AIAA Paper 2004-2923, May 2004.

[7] Liszka, L., and Waldemark, K., "High Resolution Observations of Infrasound Generated by the Supersonic Flights of Concorde," *Journal of Low Frequency Noise and Vibration*, Vol. 14, No. 4, 1995, pp. 181–192.

[8] Le Pichon, A., Garcés, M., Blanc, E., Barthélémy, M., and Drob, D. P., "Acoustic Propagation and Atmosphere Characteristics Derived from Infrasonic Waves Generated by the Concorde," *Journal of the Acoustical Society of America*, Vol. 111, No. 1, Pt. 2, Jan. 2002, pp. 629–641. doi:10.1121/1.1404434

[9] Posmentier, E. S., "Preliminary Observations of 1–16 Hz Natural Background Infrasound and Signals from Apollo 14 and Aircraft," *Geophysical Journal of the Royal Astronomical Society*, Vol. 26, 1971, pp. 173–177.

[10] Bedard, A. J., Jr., and Georges, T. M., "Atmospheric Infrasound," *Physics Today*, Mar. 2000, pp. 32–37.

[11] Balachandran, N. K., Donn, W. L., and Kaschak, G., "On the Propagation of Infrasound from Rockets: Effects of Winds," *Journal of the Acoustical Society of America*, Vol. 50, No. 2, Pt. 1, 1971, pp. 397–404. doi:10.1121/1.1912649

[12] Sutherland, L. C., and Bass, H. E., "Atmospheric Absorption in the Atmosphere up to 160 km," *Journal of the Acoustical Society of America*, Vol. 115, No. 3, Mar. 2004, pp. 1012–1032. doi:10.1121/1.1631937

[13] Locey, L., and Sparrow, V., "Atmospheric Turbulence Filter Functions Derived from High-Fidelity Measurements," *Journal of the Acoustical Society of America*, Vol. 120, No. 5, Pt. 2, Nov. 2006.

[14] Pilon, A. R., "Atmospheric Effects on Sonic Boom Loudness," *Journal of the Acoustical Society of America*, Vol. 120, No. 5, Pt. 2, Nov. 2006.

[15] Blumrich, R., Coulouvrat, F., and Heimann, D., "Meteorologically Induced Variability of Sonic-Boom Characteristics of Supersonic Aircraft in Cruising Flight," *Journal of the Acoustical Society of America*, Vol. 118, No. 2, Aug. 2005, pp. 707–722. doi:10.1121/1.1953208

[16] Plotkin, K. J., "Extension of a Sonic Boom Model to Ellipsoidal Earth

and 3-D Atmosphere," *Journal of the Acoustical Society of America*, Vol. 120, No. 5, Pt. 2, Nov. 2006.

[17] Coulouvrat, F., "Sonic Boom in the Shadow Zone: A Geometrical Theory of Diffraction," *Journal of the Acoustical Society of America*, Vol. 111, No. 1, Pt. 2, Jan. 2002, pp. 499–508. doi:10.1121/1.1371973

[18] Vermorel, J., "Extensions du Principe de Fermat à un Milieu en Mouvement," Inst. Franco-Allemand de Recherches de Saint-Louis, Rept. RT 506/87, July 1987.

[19] Johnson, D. R., and Robinson, D. W., "Procedure for Calculating the Loudness of Sonic Bangs," *Acustica*, Vol. 21, No. 6, 1969, pp. 307–318.

[20] Young, R. W., "Sonic Booms of Space Shuttles Approaching Edwards Air Force Base, 1988–1993," *Journal of the Acoustical Society of America*, Vol. 111, No. 1, Pt. 2, Jan. 2002, pp. 569–575. doi:10.1121/1.1420182

[21] Szuberla, C., Arnoult, K., and Olson, J., "Performance of an Infrasound Source Localization Algorithm," *Journal of the Acoustical Society of America*, Vol. 120, No. 5, Pt. 2, Nov. 2006.

[22] Mialle, P., Le Pichon, A., Virieux, J., and Blanc, E., "Methodology for Infrasound Sources Localization Using Global Propagation Tables," *Geophysical Research Abstracts*, Vol. 9, Feb. 2007, Paper 09096.